Blood transcriptome profiling identifies 2 candidate endotypes of atopic dermatitis

Lena Möbus, MSc,[a] Elke Rodriguez, PhD,[a] Inken Harder, MSc,[a] Nicole Boraczynski, MSc,[a] Silke Szymczak, PhD,[b] Matthias Hübenthal, PhD,[a] Dora Stölzl, MD,[a] Sascha Gerdes, MD,[a] Andreas Kleinheinz, MD,[c] Susanne Abraham, MD,[d] Annice Heratizadeh, MD,[e] Christiane Handrick, MD,[f] Eva Haufe, PhD,[g] Thomas Werfel, MD,[e] Jochen Schmitt, MD,[g] Stephan Weidinger, MD,[a] and Biomap and the TREATgermany study group *Kiel, Buxtehude, Dresden, Hannover, and Berlin, Germany*

Background: Few studies have analyzed the blood transcriptome in atopic dermatitis (AD).
Objective: We explored blood transcriptomic features of moderate to severe AD.
Methods: Blood messenger RNA sequencing on 60 adults from the TREATgermany registry including 49 patients before and after dupilumab treatment, as well as from an independent cohort of 31 patients and 43 controls was performed. Patient clustering, differential expression, correlation and coexpression network analysis, and unsupervised learning were conducted.
Results: AD patients showed pronounced inflammatory expression signatures with increased myeloid and IL-5–related patterns, and clearly segregated into 2 distinct clusters, with striking differences in particular for transcripts involved in eosinophil signaling. The eosinophil-high endotype showed a more pronounced global dysregulation, a positive correlation between disease activity and signatures related to IL-5 signaling, and strong correlations with several target proteins of antibodies or small molecules under development for AD. In contrast, the eosinophil-low endotype showed little transcriptomic dysregulation and no association between disease activity and gene expression. Clinical improvement with receipt of dupilumab was accompanied by a decrease of innate immune responses and an increase of lymphocyte signatures including B-cell activation and natural killer cell composition and/or function. The proportion of super responders was higher in the eosinophil-low endotype (32% vs 11%). Continued downregulation of *IL18RAP*, *IFNG*, and granzyme A in the eosinophil-high endotype suggests a residual disturbance of natural killer cell function despite clinical improvement.
Conclusion: AD can be stratified into eosinophilic and noneosinophilic endotypes; such stratification may be useful when assessing stratified trial designs and treatment strategies.
(J Allergy Clin Immunol 2022;150:385-95.)

Key words: *Atopic dermatitis, blood transcriptome, RNA-Seq, gene expression, dupilumab, endotypes, eosinophil signatures*

Atopic dermatitis (AD) is a highly heterogeneous disease that potentially comprises a variety of subtypes, which share common clinical characteristics but arise from distinct molecular and cellular mechanisms—that is, endotypes. Multiple skin transcriptome studies have delivered robust AD-associated

From [a]the Department of Dermatology, Venereology, and Allergology, University Hospital Schleswig-Holstein, Campus Kiel, Kiel; [b]the Institute of Medical Informatics and Statistics, University of Kiel, Kiel; [c]the Department of Dermatology, Elbe Medical Centre, Buxtehude; [d]the University Allergy Centre (UAC), Carl Gustav Carus University Medical Centre, TU Dresden, Dresden; [e]the Division of Immunodermatology and Allergy Research, Department of Dermatology, Allergology, and Venereology, Hannover Medical School, Hannover; [f]the Practice for Dermatology and Venereology, Dr med Christiane Handrick, Berlin; and [g]the Center for Evidence-based Health Care (ZEGV), Medical Faculty Carl Gustav Carus, TU Dresden, Dresden.

The TREATgermany registry currently receives independent research grants from AbbVie, LEO Pharma, Galderma, Eli Lilly, Pfizer, and Sanofi-Aventis Deutschland GmbH. Molecular profiling of an initial subgroup of TREATgermany patients was supported by a research grant of Sanofi-Aventis Deutschland GmbH. This work also received support through Biomap (Biomarkers in Atopic Dermatitis and Psoriasis), a project funded by the Innovative Medicines Initiative 2 Joint Undertaking under grant agreement 821511 and in-kind contributions of the participating pharma companies. The Joint Undertaking receives support from the European Union's Horizon 2020 research and innovation program and the European Federation of Pharmaceutical Industries and Associations (EFPIA). Infrastructure support was provided through the DFG Cluster of Excellence "Precision Medicine in Inflammation" (grant EXC2167).

Disclosure of potential conflict of interest: M. Hübenthal received project funding from LEO Pharma A/S. S. Abraham received lecture and/or consultancy fees from Novartis, LEO Pharma, Lilly, Sanofi, Beiersdorf and AbbVie. E. Haufe is an employee at the Centre for Evidence-Based Health Care at TU Dresden that received institutional support for self-designed scientific studies from ALK, Novartis, Pfizer and Sanofi. A. Heratizadeh received lecture and/or consultancy fees from LEO Pharma, Novartis, Pierre Fabre, Sanofi, Beiersdorf, Hans Karrer, Nutricia and Meda. S. Gerdes has been an advisor and/or received speakers' honoraria and/or received grants and/or participated in clinical trials of the following companies: Abbott/AbbVie, Affibody AB, Akari Therapeutics Plc, Almirall-Hermal, Amgen, Anaptys Bio, Baxalta, Bayer Health Care, Biogen Idec, Bioskin, Boehringer-Ingelheim, Celgene, Centocor, Dermira, Eli Lilly, Foamix, Forward Pharma, Galderma, Hexal AG, Incyte Inc, Isotechnika, Janssen-Cilag, Johnson & Johnson, Kymab, LEO Pharma, Medac, Merck Serono, Mitsubishi Tanabe, MSD, Novartis, Pfizer, Polichem SA, Regeneron Pharmaceutical, Sandoz Biopharmaceuticals, Sanofi-Aventis, Schering-Plough, Sienna Biopharmaceuticals, Takeda, Teva, UCB Pharma, VBL therapeutics, Wyeth Pharma. T. Werfel is co–principal investigator of the German Atopic Eczema Registry TREATgermany. He has received institutional research grants from LEO Pharma and Novartis, has performed consultancies for AbbVie, Janssen, Galderma, LEO, Sanofi-Genzyme, and Novartis. He has also lectured at educational events sponsored by AbbVie, Janssen, Celgene, Galderma, LEO Pharma, Sanofi, and Novartis, and is involved in performing clinical trials various pharmaceutical industries that manufacture drugs used for the treatment of atopic dermatitis. J. Schmitt is co–principal investigator of the German Atopic Eczema Registry TREATgermany. He has received institutional research grants for IITs from Sanofi, ALK, Novartis, and Pfizer, and has performed consultancies for Lilly, Sanofi, ALK, and Novartis. S. Weidinger is co–principal investigator of the German Atopic Eczema Registry TREATgermany. He has received institutional research grants from Sanofi Deutschland GmbH, Leo Pharma, and La Roche Posay; has performed consultancies and lectures for AbbVie, Almirall, Eli Lilly, GSK, Kymab, Leo Pharma, Pfizer, Sanofi-Genzyme, and Regeneron; and is involved in performing clinical trials with many pharmaceutical industries that manufacture drugs used for the treatment of psoriasis and atopic eczema. The other authors declare that they have no relevant conflicts of interest.

Received for publication October 28, 2021; revised January 15, 2022; accepted for publication February 3, 2022.
Available online February 16, 2022.
Corresponding author: Stephan Weidinger, MD, Department of Dermatology and Allergy, University Hospital Schleswig-Holstein, Arnold-Heller-Str 3, 24105 Kiel, Germany. E-mail: sweidinger@dermatology.uni-kiel.de.
The CrossMark symbol notifies online readers when updates have been made to the article such as errata or minor corrections
0091-6749

https://doi.org/10.1016/j.jaci.2022.02.001

Abbreviations used
AD: Atopic dermatitis
BIT: Blood-informative transcript
DEG: Differentially expressed gene
EASI: Eczema Area and Severity Index
GO: Gene Ontology (http://geneontology.org/)
LFC: Log_2 fold change
m0: Before treatment
m3: Three months after treatment
NK: Natural killer
NRS: Numeric rating score of itch
oSCORAD: Objective SCORing Atopic Dermatitis
RNA-Seq: RNA sequencing
TSLP: Thymic stromal lymphopoietin

signatures.[1-5] Those signatures reflect key and potentially shared disease mechanisms such as epidermal barrier dysfunction, activated itch signaling, and exacerbated type 2–dominated immune responses driven by skin alarmins such as thymic stromal lymphopoietin (*TSLP*), *IL33,* and *IL25,* as well as cytokines such as *IL4, IL13, IL22,* and *IL31*.[3-5] Several studies also highlighted a potential contribution of T_H17 and type 1 responses, as well as of natural killer (NK) cell signaling.[5-9]

Although skin transcriptome data are highly informative with regard to general disease mechanisms, so far, they do not resolve the heterogeneity of the disease; nor do they deliver robust biomarker signatures. Further, the limitations associated with tissue biopsies, in particular their invasiveness and sampling bias, hamper their utility as a potential method of measuring biomarkers both in the clinical setting and within trials. In contrast, blood has the advantage of being easily accessible and amenable to repetitive sampling. However, despite robust evidence for a systemic component of AD, such as altered serum protein and metabolome profiles, and reduced NK cell numbers and composition, no systematic in-depth analysis of the peripheral blood transcriptome has been performed so far.[8,10-14] A single study investigated global blood transcriptomic signatures in children with AD, although this was based on microarray data, which are less sensitive and more biased compared to RNA sequencing (RNA-Seq) data.[15] Children under the age of 6 years who had a recent AD onset showed elevated blood RNA levels of genes related to eosinophils and T_H2 cells such as *IL5RA, IL1RL1, HRH4, CCR3, SIGLEC8, PRSS33,* and *CLC,* whereas the T_H1 markers *IFNG* and *TNFA* were decreased in those patients compared to healthy controls.[15]

We here longitudinally profiled blood samples from 2 clinically and temporally well-defined cohorts to identify transcripts associated with AD and potential subtypes, and to monitor treatment response.[16]

METHODS

Patient characteristics and blood samples

Adult patients with moderate to severe AD from the TREATgermany registry recruited between August 2017 and March 2019 who agreed to participate in an optional bioanalytics module approved by the Medical Faculty of the Christian-Albrechts-University, Kiel, Germany (B 261/16), as well as the responsible local ethics committees at participating sites, were included in this study.[16] PAXgene blood samples were available from 60 patients before and from 49 patients 3 months after the initiation of a systemic therapy with dupilumab. In addition, PAXgene blood samples of 31 patients with AD as well as 43 age- and sex-matched healthy controls included in a previous skin transcriptome study under an institutional review board–approved protocol (A110/12) were available for this study.[3] In both cohorts, disease activity was assessed using established instruments, such as the Eczema Area and Severity Index (EASI), the Investigator Global Assessment, the Patient Global Assessment, the Objective SCORing Atopic Dermatitis (oSCORAD), and the itch numeric rating score (NRS).

TREATgermany is registered (VfD_TREATgermany_16_003802) in the ClinicalTrials.gov database (NCT03057860) and in the ENCePP Resource Database (European Medicines Agency).

RNA sequencing

Blood samples were stored at −80°C immediately after shipment until RNA isolation. Total RNA was isolated from PAXgene blood RNA tubes (PreAnalytiX, Hombrechtikon, Switzerland) using the PAXgene Blood miRNA Kit (PreAnalytiX) following the manufacturer's specifications automated on the QIAcube (Qiagen, Hilden, Germany). Quality control on concentration and integrity of the isolated RNA was performed with a Quant-iT fluorometer (Thermo Fisher Scientific, Waltham, Mass) and a TapeStation 4200 (RNA Screen Tape, Agilent Technologies, Santa Clara, Calif) following the manufacturer's instructions. RNA libraries were prepared for sequencing using the TruSeq Stranded messenger RNA protocol including poly-A enrichment (Illumina, San Diego, Calif). Postlibrary quality control included evaluation of library concentrations and fragment sizes (100-400 bp) on a LabChip GX (PerkinElmer, Waltham, Mass). All libraries were index barcoded, enabling multiplexed sequencing. The TREATgermany samples and the samples from the case–control cohort were randomized and sequenced together in a total of 2 sequencing runs. Samples were sequenced in pools of 37 to 40 samples per lane of an Illumina S4 flow cell on a NovaSeq 6000 machine with 2 × 100 bp, producing on average 55 million paired-end reads per sample, according to the manufacturer's protocol.

RNA-Seq data processing

The quality of the sequencing data were assessed by FastQC v0.11.5 (https://www.bioinformatics.babraham.ac.uk/projects/fastqc/). Illumina standard adapters were trimmed using Cutadapt v1.15 (parameters: minimum-length = 35, quality-cutoff = 20, overlap = 3, adapter = AGATCGGAAGAGCACACGTCTGAACTCCAGTCA-A AGATCGGAAGAGCGTCGTGTAGGGAAAGAGTGT).[17] Paired reads were mapped to the human reference genome (GRCh38, Ensembl release 99) using Tophat2 v2.1.1 and Bowtie 2 v2.3.2 (parameters: transcriptome-index yes, library-type fr-firststrand, b2-very-sensitive).[18,19] Unmapped reads were removed (parameters: view -h -F 4), and the remaining mapped reads were sorted (parameters: sort -n) using Samtools v1.5.[20] The number of reads for each gene was counted using HTSeq v0.10.0 (parameters: order name, stranded reverse, mode union, minaqual 20) and annotated according to Ensembl release 99 (http://ftp.ensembl.org/pub/release-99/gtf/homo_sapiens/Homo_sapiens.GRCh38.99.gtf.gz).[21]

Statistical analysis

In order to identify outliers—that is, samples exceptionally different from the other samples—we used the following approach. After excluding low-count genes, principal component analysis was performed for each condition: before (m0) and 3 months after (m3) treatment, AD case–control, and healthy. Principal components covering significant variance as determined by the Tracy-Widom test as implemented in the LEA Bioconductor package v3.2.0 were considered for outlier detection.[22] Samples were defined as outliers if they deviated from the mean by more than 3 times the standard deviation for at least 1 significant principal component. Outliers were excluded from all analyses. In order to identify potential batch effects due to technical variation, principal component analysis and the QCnormSE R package v0.99.2 (https://rdrr.io/github/szymczak-lab/QCnormSE/) were used. We detected batch effects between TREATgermany and the case–control cohort as well

as between different shipping times of the PAXgene tubes within TREATgermany, and applied the ComBat_seq function (Bioconductor 'sva' package v3.38.0) to remove both types of batch effects from the data.[23,24] We performed all downstream analysis using the count data with minimal but necessary correction for according batch effects.

For this study, we aimed at identifying and characterizing potential AD endotypes, their core gene signatures, and transcriptomic changes associated with systemic treatment with dupilumab. For the identification of patient subgroups, we first compiled a set of genes with the highest variances in expression in baseline (m0) AD samples denoted as AD-specific hypervariable genes.[25] We selected genes that (1) showed a variance in expression of ≥1 in the AD m0 samples, and (2) had a variance at least 2 times higher in the AD m0 samples compared to the healthy control samples. The Euclidean distance matrix was computed on the basis of those AD-specific hypervariable genes (n = 34 genes) (using normalized (DESeq2 size factor normalization) and transformed (log_2 transformation counts), and agglomerative hierarchical clustering was performed using the ward.D2 linkage criteria. The optimal number of clusters was determined using the elbow method and the silhouette score as implemented in the 'factoextra' R package v1.0.7 (https://github.com/kassambara/factoextra). In order to identify the genes underlying the cluster structure, we performed variable selection with the supervised random forest algorithm for predicting cluster membership. The Boruta algorithm as implemented in the Boruta R package was used to identify a subset of the hypervariable genes that are relevant for prediction.[26] We split the data in a training (85%) and testing data set (15%) by random sampling. We run Boruta 5 times on the training data set and used the intersect of all genes which were confirmed real predictor variables. Twenty genes yielded the "confirmed" status in all Boruta iterations (for TREATgermany m0), of which we excluded 1 uncharacterized gene (*AC025048.4)*. A random forest model was fit on the basis of the training data set using the 'caret' R package to predict the membership in 1 of the 2 clusters on the basis of the 19 predictive genes, which we termed blood-informative transcripts (BITs).[27]

To test the data on an independent test set and determine the accuracy of the cluster prediction, we ran the model on the testing data set. On the basis of 34 AD-specific hypervariable genes as determined in the TREATgermany cohort, we performed the same approach on the patients from the independent case–control cohort including hierarchical clustering of the patients, determination of the optimal number of clusters, and supervised random forest algorithm for predicting cluster membership. Of the 19 BITs as determined in the TREATgermany cohort, 17 genes could be validated as BITs by 5 Boruta iterations in the case–control cohort. Differential expression analysis was conducted by the DESeq2 Bioconductor v1.30.0 package.[28] Statistical hypothesis testing was performed by the parametric Wald test and subsequent independent filtering of the results. Differentially expressed genes (DEGs) were defined by a false discovery rate (as defined by Benjamini-Hochberg) of <5% and an absolute log_2 fold change (LFC) of >0.15 corresponding to a 10% alteration [$log_2(1.1) \approx 0.15$, $log_2(0.9) \approx -0.15$]. Because blood is a heterogenous tissue that contains a multitude of different cell types whose response to a given stimulus may vary greatly but may be diluted, and because in this study a measurement technology was applied that also allows detection of transcripts with small fold changes, we analyzed the data deliberately using a more liberal threshold in order to also capture smaller differences in gene expression that may still be biologically relevant. Log fold change estimates were corrected by the DESeq2 inbuilt LFC shrinkage function with the 'apeglm' method.[29] Differential expression analysis of patients versus healthy controls was conducted across both cohorts after batch correction. Enrichment tests of DEGs were conducted using the overrepresentation analysis of Gene Ontology (GO; http://geneontology.org/) biological processes with default parameters as implemented in the Clusterprofiler Bioconductor v3.18.0 package.[30] Coexpression network analysis was performed by INfORM software with fragments per kilobase per million mapped fragments of the DEGs as input.[31] We used default INfORM settings except that we omitted the 'mrnetb' algorithm to speed up the computation of the network. For the calculation of fragments per kilobase per million mapped fragments values, the size-factor-normalized counts were additionally normalized for gene length using the 'fpkm' function implemented in DESeq2.[28] For network analysis of the eosinophil-high endotype versus healthy controls, we included DEGs with an absolute LFC of >0.5 to speed up the computation and for better visualization. For gene–gene or gene-variable correlation analysis, we performed Spearman rank-based correlation using normalized (DESeq2 size factor normalization) and transformed (log_2 transformation) sequencing counts. We used the Human Protein Atlas to explore cell type specificity of gene expression.[32] For descriptive statistics and visualization, normalized (DESeq2 size factor normalization) and transformed (log_2 transformation) gene counts were used.[28]

Differences in clinical variables were tested by the chi-square test for categorial and the Wilcoxon signed rank test for numeric variables and ordinal categorial variables. All analyses were performed by R v4.0.3 and Bioconductor v3.12.

RESULTS

After quality control, whole-blood transcriptome data were available from 56 AD patients at m0 from the TREATgermany registry. Forty-six of those patients had received treatment with dupilumab, and m3 transcriptome data were available for 42 of those patients. Response rates for EASI50, EASI75, and EASI90 at m3 were 85%, 61%, and 24%, respectively. From the AD case–control cohort, whole-blood transcriptome data were available from 31 patients and 40 healthy controls. The baseline characteristics of the study participants are shown in Table I. The patients from the case–control cohort had a higher proportion of female subjects, a lower mean age, and lower age at disease onset as well as a lower mean disease activity as measured by the oSCORAD and Investigator Global Assessment tools compared to the group of patients from the TREATgermany registry.

AD patients exhibit inflammatory gene expression signatures with increased myeloid and IL-5–related pattern in peripheral blood

Transcriptome-wide differential expression analysis of all 87 AD patients and 40 healthy controls revealed 622 DEGs, with 301 and 321 genes showing up- and downregulation, respectively (see Table E1 in this article's Online Repository at www.jacionline.org). The top significant DEGs were *IGHE, CCL23,* and *IL34* (upregulated) and *ZNF774, JCHAIN,* and *PLAAT2* (downregulated) (Fig 1, *A*). Except for *IL13,* which showed a slight upregulation (nonsignificant), important cutaneous type 2 cytokines and their receptors, including *IL4, IL4RA, IL13RA1, IL31, IL31RA1,* and *TSLP,* did not show relevant dysregulation (see Fig E1 in the Online Repository). On the functional-group level, genes downregulated in AD were enriched for humoral immune response, immunoglobulin production, regulation of B-cell proliferation and activation, and lymphocyte-mediated immunity, which is in line with our observations on the single-gene level with downregulations of multiple genes encoding immunoglobulin chains as well as *CCR6, IL23A, CD38, MZB1, TNFRSF4,* and *TNFRSF13B* (Fig 1, *B;* see Table E2 in the Online Repository). In contrast, upregulated genes were enriched for processes such as myeloid leukocyte differentiation and IL-5 production, as reflected on the single-gene level by upregulations of *IL34, PRTN3, CSF1, CD109,* and *VEGFA,* as well as *IL5RA*, *IL1RL1, EPX,* and *CRLF2.* We checked whether these genes are also dysregulated in AD skin lesions using recently published data from a subset of the patients analyzed in the current study.[5] Some of the genes upregulated in blood, such as *CCL23, CSF1, IL5RA,* and *IL1RL1,* displayed an increased expression also in skin lesions, but with relatively small fold changes. At the same time, some genes downregulated in blood, such as *JCHAIN, CCR6, IL23A,* and *TNFRSF4,* showed an upregulation in skin lesions, while others

TABLE I. Clinical characteristics of patients

Characteristic	TREATgermany case-control cohort		
	Patients (n = 56)	Patients (n = 31)	Controls (n = 40)
Female sex	16 (28.6)	15 (48.4)	21 (52.5)
Age (years), mean ± SD	44.4 ± 14.2	31.6 ± 10.3	32.4 ± 11.4
Body mass index (kg/m^2), mean ± SD	26.8 ± 4.6	26.5 ± 6.8	24.0 ± 4.2
oSCORAD	44.1 ± 13.4	30.1 ± 10.8	—
EASI, mean ± SD	20.7 ± 11.0	—	—
IGA, mean ± SD	3.7 ± 0.7	2.5 ± 0.9	—
PtGA, mean ± SD	3.5 ± 1.0	—	—
Pruritus past-week NRS, mean ± SD	6.3 ± 2.3	5.0 ± 1.9	—
Age (years) at onset, mean ± SD (min, max)	9.4 ± 17.7 (0, 77)	4.5 ± 5.7 (0, 22)	—
Topical corticosteroid therapy at baseline	52 (93)	29 (94)*	—
Physician-diagnosed asthma	36 (64.3)	18 (58.1)	0
Medicated at m0	33 (92)	—	—
Medicated at m3	33 (92)	—	—
Physician-diagnosed rhinitis	41 (73.2)	17 (54.8)	0

Data are presented as nos. (%) unless otherwise indicated.
IGA, Investigator Global Assessment; *PtGA,* Patient Global Assessment.
*No topical treatment within 1 week before material sampling.

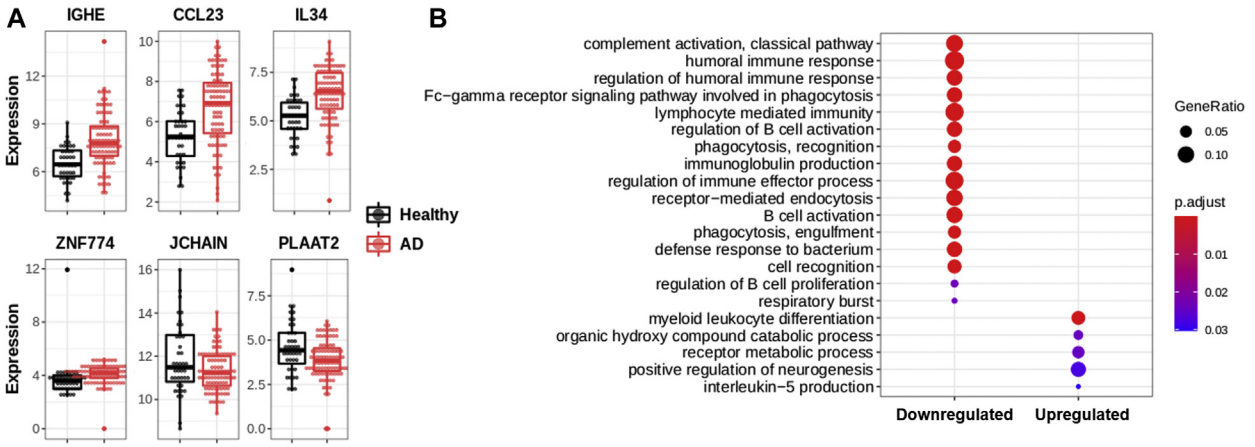

FIG 1. Dysregulation of AD compared to healthy controls. **A**, Expression of top significantly up- and downregulated genes in AD (n = 87) compared to healthy controls (n = 40). Gene expression is depicted in terms of $\log_2$ sequencing counts. **B**, GO gene group enrichment analysis with the DEGs detected in AD compared to healthy controls. For this analysis, DEGs were separated in up- and downregulated genes, respectively. Selected biological processes from the top enriched processes are shown. Color code shows the *P* value of the enrichment; dot size indicates the gene ratio (ie, the number of genes matching the GO term divided by the total number of DEGs).

were not even detectable in skin. Thus, expression changes in blood do not simply reflect changes resulting from skin inflammation.

We performed a transcriptome-wide correlation analysis of gene expression with AD activity as measured by oSCORAD, EASI, and itch NRS. After correction for multiple testing, 7 protein-coding genes showed a significant correlation with the oSCORAD (Spearman ρ ranging from −0.47 to 0.5): *IL2RA, GPR52, MEOX1, TRNP1, ARSB, PRR11,* and *PRSS22* (see Fig E2 and Table E3 in the Online Repository at www.jacionline.org).

Blood transcriptome profiles separate AD patients into an eosinophil-high and eosinophil-low endotype

In order to identify potential disease endotypes, we first determined AD-specific hypervariable genes across the TREATgermany patients. We identified 34 genes corresponding to the top 1.4% variable genes, with *ALOX15, ADAMTS2, CCL23,* and *IGHE* showing the highest variance (see Fig E3, *A,* in the Online Repository at www.jacionline.org). On the basis of the expression of these 34 genes, we performed a hierarchical clustering with an optimal number of 2 clusters (Fig E3, *B-D*). Using a machine learning approach, we determined a subset of 19 BITs that classified patients in the 2 clusters with an accuracy of 1 (Fig 2). The 2 clusters showed striking differences in the expression levels of genes highly specific for eosinophils/eosinophil signaling, such as *IL5RA, CCL23, IL34, SIGLEC8, SLC29A1, PRSS33,* and *PTGDR2*. We therefore termed the 2 identified clusters as being an eosinophil-high (n = 23 patients) or eosinophil-low (n = 33 patients) endotype. Transcriptome-wide differential expression analysis between the 2 endotypes showed a total of 548 genes with significant differential expression and confirmed the upregulated expression of *IL5RA, CCL23, IL34,* and

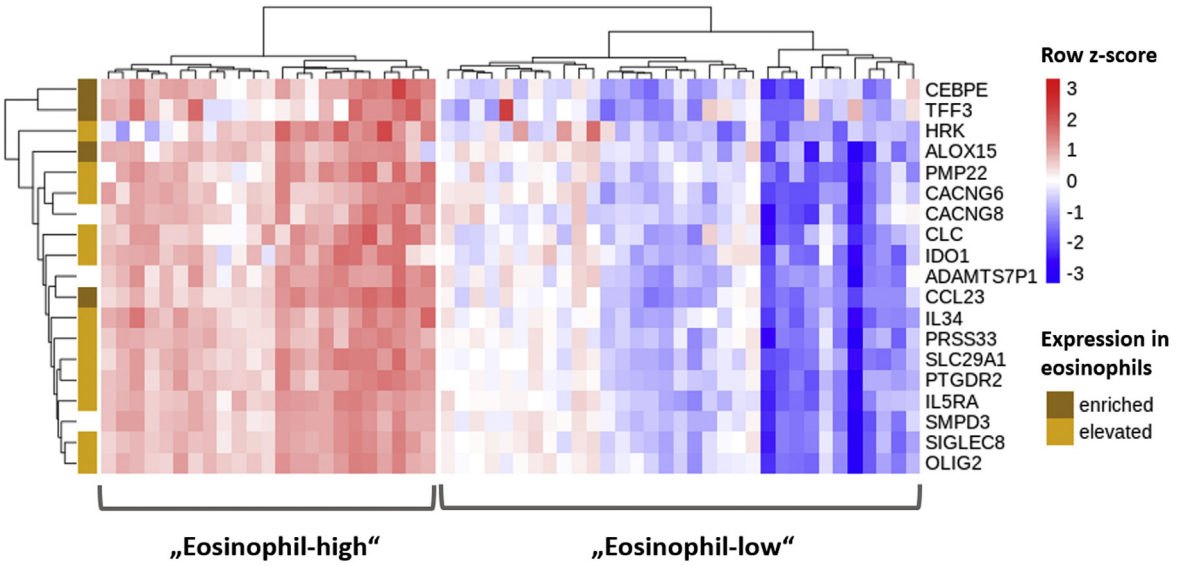

FIG 2. Clustering of TREATgermany m0 AD samples. Hierarchical clustering of 56 m0 AD samples based on the expression of 34 AD-specific hypervariable genes grouped the patients in an eosinophil-high and an eosinophil-low endotype. On the basis of a subset of 19 of 34 hypervariable genes, the patients were classified according to the 2 endotypes with an accuracy of 1. The vertical *yellowish* color bar shows the cell-type specificity for eosinophils according to the Human Protein Atlas with *enriched* indicating genes that show an enriched expression in esosinophils and *elevated* indicating genes with elevated expression in eosinophils (*enriched* is superior to *elevated*). The heat map color code represents row *z* scores.

ALOX15 in the eosinophil-high endotype (see Fig E4 and Table E4 in the Online Repository). In addition, further genes with specific expression in eosinophils and/or basophils such as *HRH4, CCR3, EPX, HSD3B7, RNASE2, IL3RA, IL1RL1,* and *SOCS1* were upregulated in the eosinophil-high endotype.

In order to validate our observations, we performed a clustering on the basis of the 34 identified AD-specific hypervariable genes of the AD patients in the independent case–control cohort. Like the TREATgermany cohort, patients clustered in an eosinophil-high and eosinophil-low endotype. Of the 19 BITs determined as the minimal predictive gene set for the TREATgermany cohort, a subset of 17 genes could be validated as BITs in the independent case–control cohort, and patients could be classified into the 2 clusters as given by hierarchical clustering with an accuracy of 1 on the basis of those 17 BITs (see Fig E5 in the Online Repository at www.jacionline.org). No significant overlap was seen of BITs identified in a cohort of 28 psoriasis patients[3] and the 17 BITs identified in the AD cohort analyzed here, indicating that the identified BITs are specific for AD.

Transcriptome-wide differential expression analysis comparing patients with an eosinophil-high endotype (n = 46 patients) and healthy controls (n = 40) revealed 1002 DEGs, with 562 genes showing upregulation and 440 genes showing downregulation (see Table E5 in the Online Repository at www.jacionline.org). The top upregulated genes in the eosinophil-high endotype were those genes that also differentiated the 2 endotypes such as *IL34, CCL23, IL5RA,* and *HRH4,* as well as *IL13* (Fig 3, *A*). Downregulated transcripts included *IL18RAP* and *KLRC1* (NKG2A), both of which have a high specificity for NK cells (Fig 3, *A*). Several genes primarily expressed by lymphoid cell lines such as T cells, B cells, and NK cells showed a considerably stronger dysregulation in the eosinophil-high endotype including the upregulated genes *IGHE, CCR10,* and *IL17RB* as well as the downregulated genes *TNFRSF4* (OX40), *IL7R, CCR6,* and *KLRB1* (CD161) (Fig 3, *B*). In contrast, the eosinophil-low endotype (n = 41 patients) showed only 33 DEGs, indicating a considerably lower global transcriptomic dysregulation in blood (see Table E6 in the Online Repository). However, genes such as *CD34, FOSB, IGLL1,* and *ECRG4* showed a stronger degree of dysregulation in the eosinophil-low endotype (Fig 3, *C*). Genes that showed a comparable dysregulation in both endotypes comprised, for example, the neutrophil-related *PI3* (elafin) and *PRTN3,* as well as *APOL4* (upregulated), and *IL23A* and the NK cell–related genes *KLRF1,* encoding an activating receptor on NK cells, and *GZMA* (downregulated) (Fig 3, *D*). On the functional level, genes downregulated in the eosinophil-high endotype were enriched for lymphocyte-mediated immunity, humoral immune responses, and B-cell–related processes, as well as for NK cell–mediated cytotoxicity, supporting our observations on the single-gene level with downregulations of *TNFRSF4, IL7R, CCR6, IL23A* (B and T lymphocytes), and *IL18RAP, KLRC1,* and *KLRF1* (NK cells) (Fig 3, *E*). In contrast, upregulated genes in the eosinophil-high endotype were enriched for processes related to neutrophil differentiation, as is also reflected on the single-gene level by upregulations of the neutrophil-related genes *PI3* (elafin) and *PRTN3*. We further examined the expression of selected genes known to be dysregulated in the skin of patients with AD. Except for *IL13,* which showed significant upregulation in the eosinophil-high endotype, no other type 2 marker, including *IL4, ILRA, IL3RA1, IL1RA,* and *TSLP,* showed a relevant dysregulation compared to healthy controls (see Fig E6 in the Online Repository).

Full blood counts and differential blood counts were available from 19 of 56 TREATgermany patients (8 and 11 from the eosinophil-high and -low endotype, respectively). In this small subset, the 2 endotypes did not differ significantly with regard to

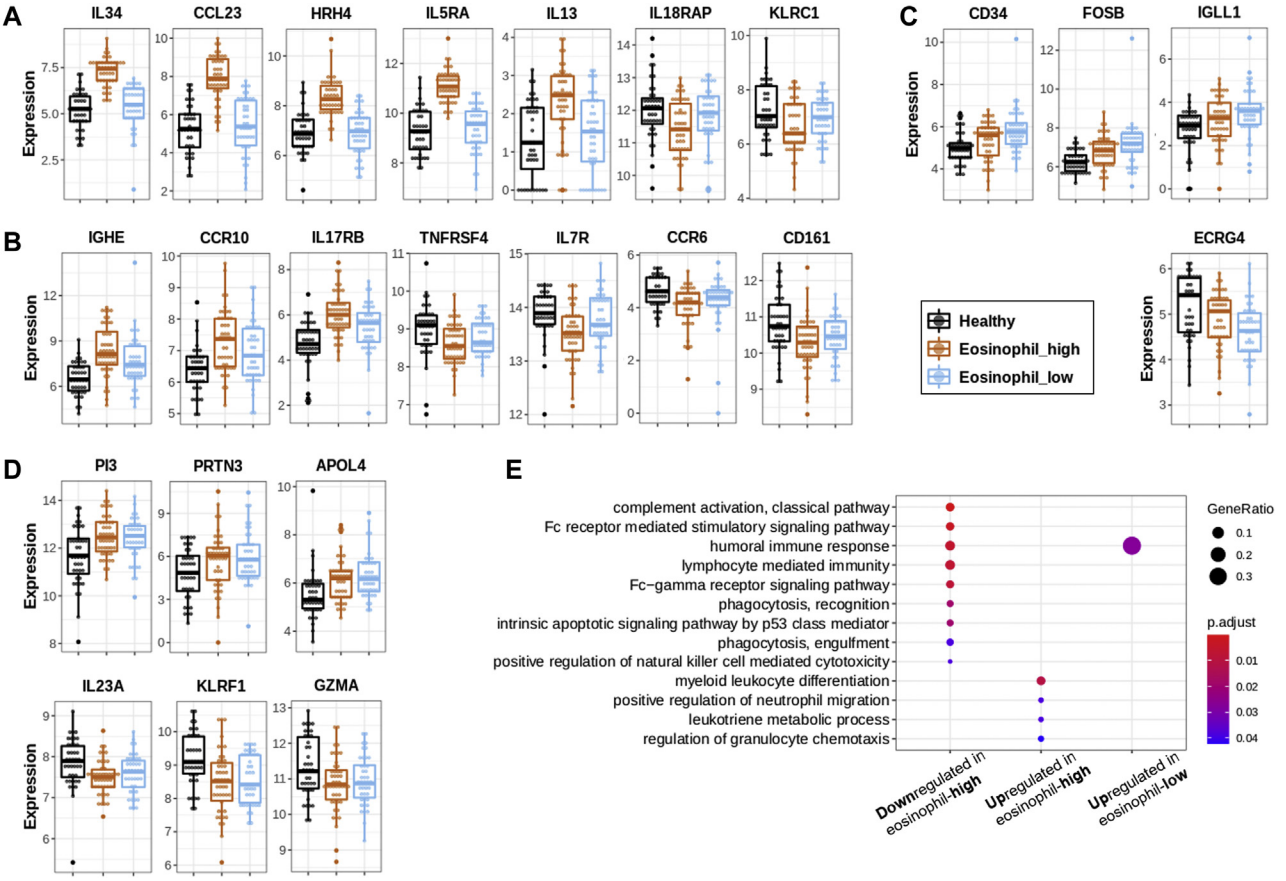

FIG 3. Dysregulation in AD endotypes compared to healthy controls. **A**, Expression of genes that were dysregulated solely in the eosinophil-high endotype (n = 46 patients) compared to healthy controls (n = 40 individuals). Gene expression is depicted in terms of $\log_2$ sequencing counts. **B**, Genes that showed a higher degree of dysregulation in the eosinophil-high endotype compared to the eosinophil-low endotype (n = 41 patients). **C**, Genes that showed a higher degree of dysregulation in the eosinophil-low endotype compared to the eosinophil-high endotype. **D**, Genes that showed a comparable dysregulation in both endotypes compared to healthy controls. **E**, GO gene set enrichment analysis with the DEGs detected in both endotypes compared to healthy controls. For this analysis, DEGs were separated into up- and downregulated genes, respectively. There were no significantly enriched terms identified for the downregulated genes in the eosinophil-low endotype. Color code shows the *P* value of the enrichment; dot size indicates the gene ratio (ie, the number of genes matching the GO term divided by the total number of DEGs).

leukocyte, lymphocyte, neutrophil, monocyte, eosinophil, or basophil numbers and proportions, although eosinophil proportions were slightly higher in patients assigned to the eosinophil-high endotype (mean 12.5% vs 6.5%, adjusted P = .39).We observed neither marked nor significant differences between the endotypes with regard to obvious clinical characteristics at baseline, including frequency of comorbidities, except for slightly higher itch intensity reported by patients of the eosinophil-high endotype (median itch NRS 7 vs 5). An analysis of a subset of patients with total and specific IgE values available indicated higher total IgE levels in the eosinophil-low group but found no difference with regard to the number or pattern of specific sensitizations (Table II). A transcriptome-wide analysis showed no marked correlation between gene expression and disease activity as measured by the oSCORAD for the eosinophil-low endotype; however, 222 genes (Benjamini-Hochberg adjusted $P < .05$) were significantly correlated in the eosinophil-high endotype (see Tables E7 and E8 in the Online Repository at www.jacionline.org). Interestingly, in the eosinophil-high but not eosinophil-low endotype, oSCORAD and itch NRS were positively correlated with the expression levels of *CCL23, IL5RA,* and *HRH4* (see Fig E7 in the Online Repository). Of note, *CSF2RB,* which together with *IL5RA* encodes the IL-5 receptor heterodimer, was among the top correlated genes (Spearman $\rho = 0.82$), supporting the correlation between disease activity and *IL5RA* expression in patients of the eosinophil-high endotype.

Coexpression network and drug–target interaction analysis

Coexpression network analysis including a ranking of the genes by the combined influence of network centrality properties and differential expression scores identified *PIK3R6, CEBPE,* and *SPNS3* as the top central genes across all patients, and *SLC29A1, PIK3R6,* and *IL34* as the top 3 central genes in the eosinophil-high endotype (see Tables E9 and E10 in the Online Repository at www.jacionline.org). Other highly ranked genes in the eosinophil-high endotype included *IL5RA, PTGDR2,* and *CCL23* (Table E10). We correlated the top 30 central genes of

TABLE II. TREATgermany eosinophil-high and eosinophil-low patient characteristics

Characteristic	Eosinophil-high (n = 23)	Eosinophil-low (n = 33)	*P* value
Age (years), mean ± SD	44.09 ± 13.72	44.67 ± 14.67	.65*
Female sex, no. (%)	7 (30.4)	9 (27.3)	1†
Body mass index (kg/m^2), mean ± SD	28.03 ± 5.72	25.96 ± 3.51	.15*
oSCORAD, mean ± SD	46.21 ± 13.51	42.60 ± 13.31	.23*
EASI, mean ± SD	22.35 ± 12.01	19.61 ± 10.35	.44*
IGA, mean ± SD	3.74 ± 0.69	3.61 ± 0.70	.96†
Itch NRS, mean ± SD	6.91 ± 2.09	5.88 ± 2.34	.08*
Age at AD onset (years), mean ± SD	8.48 ± 17.64	9.94 ± 17.94	.59*
Serum IgE (IU/mL), mean ± SD‡	3144.67 ± 2272.6	5382.45 ± 6442.99	1*
Diagnosis asthma			.25†
No	6 (26.1)	14 (42.4)	
Yes	17 (73.9)	19 (57.6)	
Diagnosis rhinitis			1†
No	6 (26.1)	9 (27.3)	
Yes	17 (73.9)	24 (72.7)	
Asthma/rhinitis			.61†
None	4 (17.4)	7 (21.2)	
One	4 (17.4)	9 (27.3)	
Both	15 (65.2)	17 (51.5)	
Sensitization pollen			.7†
No	4 (17.4)	4 (12.5)	
Yes	18 (78.3)	27 (84.4)	
Sensitization dust mite			1†
No	3 (13.0)	5 (15.6)	
Yes	19 (82.6)	25 (78.1)	
Sensitization food			.12†
No	6 (26.1)	17 (53.1)	
Yes	11 (47.8)	10 (31.2)	

Data are presented as nos. (%) unless otherwise indicated. *IGA,* Investigator Global Assessment.
*By Wilcoxon test.
†By chi-square test.
‡Available from a subset of patients (n = 26) only.

the consensus networks with 9 specific target proteins of monoclonal antibodies or small molecules under development for AD (IL4RA, IL13, IL13RA1, IL5RA, IL31RA, TNFRSF4 [OX40], TNFSF4 [OX40L], HRH4, and TSLP) (Fig 4, A and B). Further target proteins such as IL5, IL22, and IL31 showed a too low gene expression to be included into this analysis. For the eosinophil-high endotype, the strongest correlation with the top central genes was seen for *IL5RA* and *HRH4* (mean ρ *IL5RA* = 0.83; mean ρ *HRH4* = 0.76) (Fig 4, *B*). *IL5RA* was a central gene, which explains the high correlation of the top central genes with it. Clearly weaker correlations were seen with IL13 (mean ρ = 0.28) and IL4RA (mean ρ = 0.27), and very weak correlations only with OX40L (mean ρ = 0.15), IL13RA1 (mean ρ = 0.12), TSLP (mean ρ = 0.1), IL31RA (mean ρ = 0.08), and OX40 (mean ρ = 0.05). Because the eosinophil-low endotype revealed only about 30 DEGs in total, no network analysis was performed. Instead, we correlated all identified DEGs with the 9 therapy targets, detecting only low correlations for *IL5RA* and *HRH4* compared to the eosinophil-high endotype (Fig 4, *C*).

Blood transcriptome changes with receipt of dupilumab treatment indicate a downregulation of neutrophil signatures and an activation of B cells and elevation of NK cells

Blood transcriptome data sets before and 3 months after initiation of treatment with dupilumab were available from 42 patients. Across these patients, the mean oSCORAD and EASI reductions were 51% and 74%, respectively. Patient-wise paired differential expression testing showed expression changes for 347 genes (306 genes downregulated, 41 genes upregulated; see Table E11 in the Online Repository at www.jacionline.org). The most pronounced changes were seen for the *IGHE* gene encoding the constant region of the IgE heavy chain (LFC −1.8, 70% reduction) as well as *KLRF1* (Nkp80) (LFC 0.44, 36% increase) and *KLRC2* (NKG2C) (LFC 0.40, 32% increase), both of which encode activating NK cell receptors. However, the expression of these genes did not correlate with total IgE levels. Coexpression network and network community analysis based on the DEGs at m3 versus m0 identified 4 modules of highly intercorrelated genes (Fig 5). The largest module, mainly consisting of downregulated genes, was enriched for innate immune response processes such as neutrophil activation and macrophage differentiation and included genes such as *LILRA2, IL1RN, MMP9, PRTN3, OSM, BCL3, ORM1,* and *S100A11* (see Table E12 in the Online Repository). Two additional modules consisting of downregulated genes were enriched for processes related to mitotic cell cycle as well as general metabolic processes and GO terms such as "drug response" (see Tables E13 and E14 in the Online Repository). The smallest module consisted of upregulated genes only and was enriched for B-cell activation and humoral immune response by genes such as *BANK1, FCRL1, MS4A1,* and *BLNK* (see Table E15 in the Online Repository). Across all patients, gene expression changes observed during receipt of therapy were not robustly correlated with the degree of clinical improvement, such as changes of oSCORAD or

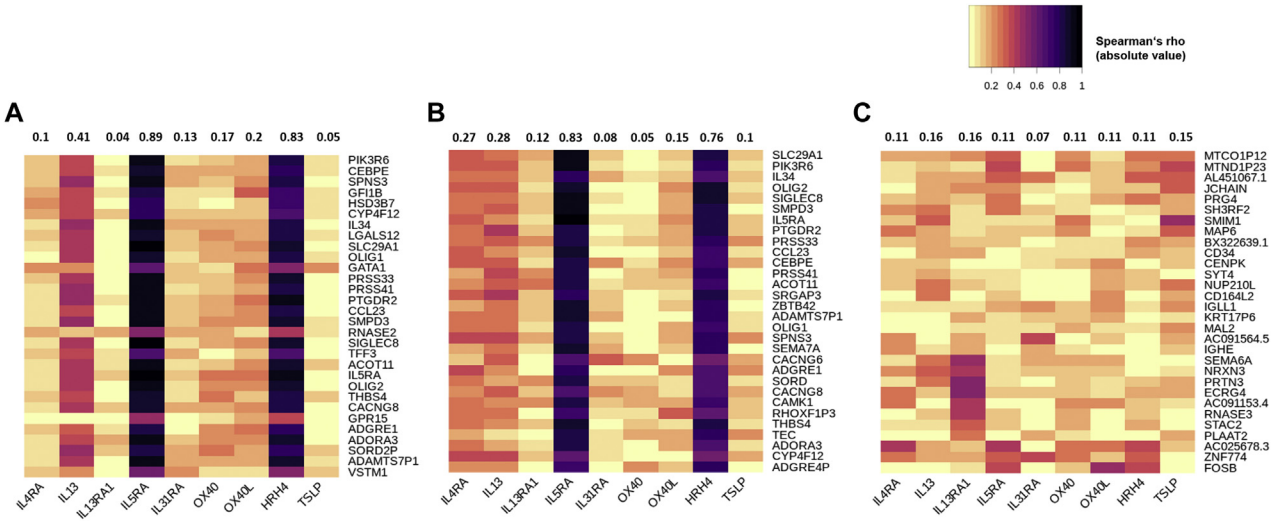

FIG 4. Central genes in a coexpression network and their relation to (potential) therapeutic targets. **A**, AD vs healthy controls. The top 30 central genes from the coexpression network analysis and their correlation with genes that can be blocked by targeted treatments that have been or are currently evaluated in clinical trials of AD. **B**, Eosinophil-high endotype vs healthy controls. The top 30 central genes from the coexpression network analysis and their correlation with genes that can be blocked by targeted treatments. **C**, Eosinophil-low endotype vs healthy controls. All identified DEGs and their correlation with genes that can be blocked by targeted treatments. Heat map color code represents Spearman ρ (absolute value). The numbers on *top* of the heat maps represent column mean ρ. In (*A*) and (*B*), the genes were ranked (top down) by the combined influence of network centrality properties and differential expression scores.

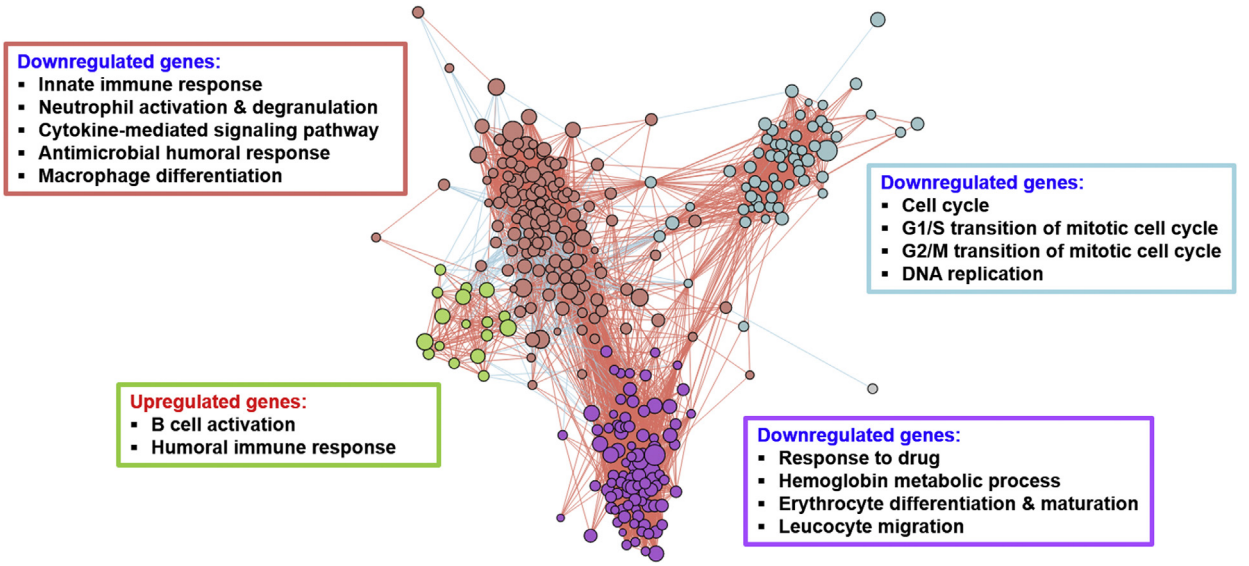

FIG 5. Changes during receipt of dupilumab on coexpression and functional group level. Coexpression network was computed on the basis of the DEGs in blood from the comparison of m3 and m0. Community detection identified 4 modules of genes within the network. Functional gene set enrichment analysis using GO terms was carried out for each module.

EASI. However, the sample size and the variability with regard to response were rather low.

Of the 42 patients treated with dupilumab, 16 and 26 patients were assigned to the eosinophil-high and eosinophil-low endotype, respectively. Overall, the eosinophil-high endotype showed considerably more expression changes with receipt of dupilumab treatment, with 40 genes showing upregulation and 137 showing downregulation (see Table E16 in the Online Repository at www.jacionline.org). In the eosinophil-low endotype, only 12 DEGs were identified, all showing downregulation (see Table E17 in the Online Repository). In the eosinophil-high endotype, the majority of genes that showed particularly strong upregulation at baseline such as *IL5RA, IL34, CCL23, HRH4,* and *IL3* showed little or no changes during receipt of therapy with dupilumab and no correlation with treatment response, indicating that the endotype structure is largely stable despite clinical improvement (see

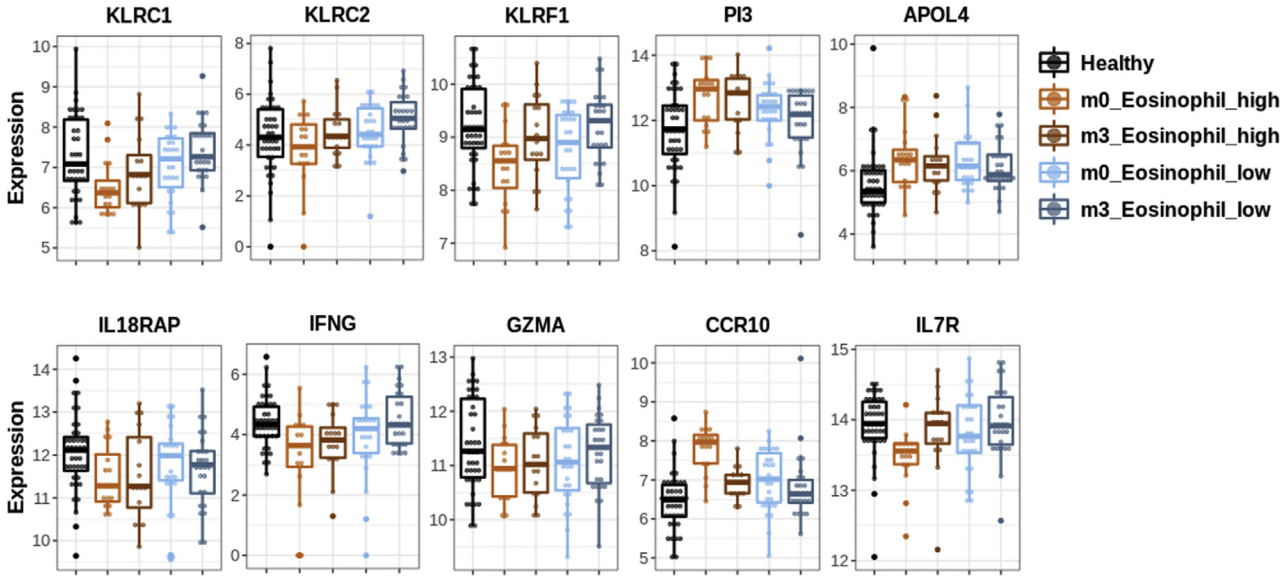

FIG 6. Blood transcriptomic changes during receipt of dupilumab. Gene expression of selected genes in healthy controls, AD patients at baseline (m0) as well as AD patients 3 months after the start of treatment with dupilumab (m3), separated into eosinophil-high and eosinophil-low endotypes, respectively. Gene expression is depicted in terms of $\log_2$ sequencing counts.

Fig E8 in the Online Repository). For both endotypes, we observed a normalization of the downregulated expression of *KLRC1, KLRC2,* and *KLRF1* encoding an inhibitory and 2 activating receptors primarily expressed by NK cells during treatment in both endotypes—that is, a normalization of NK transcriptomic signatures (Fig 6). In contrast, several genes downregulated at m0 such as *PI3* and *APOL4* remained dysregulated at m3 in both endotypes, indicating a residual inflammatory expression pattern. In patients of the eosinophil-high endotype, *IL18RAP, GZMA,* and *IFNG* expression also remained downregulated, suggesting a residual disturbed *IFNG* expression by NK and T_H1 cells in patients of this cluster (Fig 6). Expression of the T-cell–related genes *IL7R* and *CCR10* showed a baseline dysregulation especially in the eosinophil-high endotype, and within 3 months of treatment, the expression of *IL7R* and *CCR10* markedly normalized in the eosinophil-high endotype.

Overall, we did not detect marked differences between the endotypes with regard to response to dupilumab treatment. However, super responders, defined as having an EASI90 at m3 or a Patient Global Assessment score of 0 or 1 at month 6 were slightly overrepresented in the eosinophil-low endotype (32% vs 11%, 9/28 vs 2/18 and 62.5% vs 25%, 10/16 vs 4/16, respectively).

DISCUSSION

It is widely recognized that AD is a highly heterogenous disease with wide variations in clinical features, course, and response to therapy, and that the current broad and inclusive concept of AD probably encompasses distinct subtypes with a varying relative importance of different and interacting pathomechanisms. With the availability of an increasing number of therapeutics targeting specific pathways involved in AD, understanding disease relevant subtypes and their molecular underpinnings along with associated biomarker signatures that could guide the selection and application of therapeutics is therefore becoming increasingly important. Transcriptomic and proteomic profiling of biopsies has delivered important insights into general disease mechanisms in the skin, but has so far not delivered robust endotypes or biomarkers that would allow a stratification of patients. The results of this first large-scale analysis of the blood transcriptome show that moderate-to-severe AD has a strong systemic inflammatory component and provides evidence for blood biomarker-based endotypes.

The "eosinophil-high" endotype representing 53% of the patients studied in this work is characterized by a strongly elevated eosinophil-related expression signature and shows a high degree of global transcriptomic dysregulation. In contrast, the eosinophil-low endotype displays a rather low degree of transcriptome dysregulation and has no marked eosinophil-related expression signature, and might designate a subgroup of patients that lack a marked systemic transcriptomic dysregulation of proinflammatory genes. However, both endotypes showed a comparable mean disease activity at recruitment.

Although results from routine blood testing were available only from a subset of patients, both clusters did not exhibit significant differences with regard to eosinophil numbers, and expression differences did not show a clear correlation with individual cell numbers indicating that the strikingly different expression of eosinophil signaling genes might rather be driven by cellular activation. Although the 2 candidate endotypes differ in the expression levels of as many as 548 genes, a signature of only 19 hypervariable genes was sufficient to reliably classify patients into the clusters. Interestingly, only patients of the eosinophil-high endotype showed an upregulation also of genes that were recently reported to be upregulated in children with recent AD onset such as *CCL23*, *IL5RA*, *IDO1*, *HRH4*, *CCR3*, *CLC*, *SIGLEC8*, *ALOX15*, *PTGDR2*, and *PRSS33*.[15]

The 2 endotypes did not show marked differences with regard to the clinical variables studied nor the overall response to

treatment with dupilumab, although the proportion of super responders was slightly higher in the eosinophil-low endotype. While blood transcriptomic signatures of AD overall not readily reflect cutaneous signatures,[1,2,5] heightened type 2 responses are seen in both tissues,[3,5] which might explain why most patients, irrespective of their endotypes, appear to benefit at least to some extent from directly inhibiting key cytokines of type-2 signaling.[10] In fact, across patients treated with dupilumab, we observed a shift of the blood transcriptome indicating a downregulation of innate immune signaling and an increase of NK cell abundance along with a functional shift of NK cells. However, there was a largely stable downregulation of *GZMA, IL18RAP,* and *IFNG* in the eosinophil-high endotype, which might reflect a residual dysregulation and disturbed cytotoxic effector function of killer cells.[32,33] Interestingly, the characteristic gene expression of the eosinophil-high endotype centered around IL-5 signaling was persistent despite clinical improvement during receipt of therapy with dupilumab, indicating that the endotype structure according to eosinophil transcriptomic signatures is stable and/or reflects activated pathways that are not affected by IL4RA blockade.

The top central genes of the eosinophil-high coexpression network are *IL5RA, HRH4,* and *PTGDR2/CRTH2,* all of which are targets of drugs being developed for AD. While the anti–IL5RA antibody benralizumab is currently in a phase 2a study in AD (HIL-LIER Study, NCT04605094), early phase studies on the anti–IL-5 antibody mepolizumab, the H4R antagonist adriforant, and the CRTH2 antagonists fevipiprant and temapiprant (OC000459) showed only moderate effects on the AD patient population at large.[34] Thus, it might be speculated that subgroups of patients, such as those with an eosinophil-high endotype, benefit more from approaches targeting eosinophil signaling, such as the IL-5 pathway, or from adding such treatments. This will have to be tested in future trials. Likewise, with increasing numbers of AD patients being treated with Janus kinase inhibitors, it will be interesting to study responses to these rather broad immunomodulators on the transcriptomic level and with regard to the proposed endotypes. We also observed dysregulations across the endotypes, which reflect elevated neutrophil as well as inflammatory and innate immune signaling and affect genes such as *PI3* and *PRTN3.* In contrast, signatures related to lymphoid cells, in particular NK and related cytotoxic killer cells overall, were diminished in AD, as reflected by a downregulation of genes such *KLRF1, GZMA, KLRC1, IL18RAP,* and *IFNG. KLRF1,* which showed the strongest downregulation, encodes NKp80, an activating receptor stimulating NK cell cytotoxicity and cytokine release.[33] Further, NKp80 is a marker of NK cell maturity. While NKp80$^-$ cells represent a more immature stage, NKp80$^+$ NK cells produce IFNG and are cytotoxic. This suggests that circulating NKp80$^+$ NK cells are reduced in AD.[35] Thus, the downregulation of *IL18RAP* and *GZMA,* which have a high specificity for NK cells, as well as *IFNG,* is coherent with the downregulation of *KLRF1* (NKp80).[32,36] Our observations are consistent with recent reports about decreased peripheral NK cell numbers in patients with AD, and they further emphasize a selective reduction of certain killer cell subpopulations that express NKp80 because other NK cell markers such as CD56, CD16A (FCGR3A), CD94 (KLRD1), and NKG7 showed no downregulation by our data.[8] However, cell-based and transcriptomic studies on the single-cell level are urgently needed in order to better understand the role of NK cells in the pathophysiology of AD.

Besides *IL5RA, CSF2RB* encoding the other heterodimer of the IL5 receptor showed a strong correlation with disease activity in the eosinophil-high endotype, although *CSF2RB* itself was not dysregulated. This indicates that stratification of patients on the basis of molecular mechanisms may aid the detection of biomarkers, and that surrogate markers for relevant clinical variables are not necessarily associated with the disease itself.

Our study has several strengths, such as the use of 2 stringently recruited and well-phenotyped patient cohorts, the application of sensitive and transcriptome-wide RNA-Seq, and the use of unsupervised but straightforward analytical approaches. Although the use of PAXgene whole blood instead of the peripheral blood mononuclear cell fraction limits the analytical depth of immune cell signatures as a result of high abundant transcripts from erythrocytes and reticulocytes, we compensated for this by an exceptional sequencing depth of 55 Mio reads per sample. Further, whole-blood sequencing has advantages over peripheral blood mononuclear cell sequencing, such as capturing all blood cell populations including granulocytes, as well as a lower variability and higher sensitivity, which is relevant for multicenter studies.[37-39] Our study, however, suffers from limitations related to whole-blood RNA sequencing such as the low coverage of relevant immune mediators such as IL4, IL5, and CCL17, and from an overall relatively low sample size. Independent longitudinal studies will improve our understanding of the robustness of the 2 candidate endotypes and the true clinical value of the proposed peripheral blood transcriptomic signatures. Further, while differential messenger RNA expression is suitable for biological discovery, additional analysis on the protein and single-cell level will be needed to better understand if and to what extent the transcriptome patterns observed in this study translate into altered protein expression, and which cells are involved.

We thank all participating patients and all study physicians and study staff in the participating clinics and offices for their support of the German Atopic Dermatitis Registry TREATgermany.

Key messages

- **Blood transcriptome analysis indicates 2 AD endotypes which differ in the expression levels of genes specific for eosinophils/eosinophil signaling.**
- **Treatment with dupilumab leads to a downregulation of innate immune system signatures and an upregulation of NK cell and other cytotoxic killer cell signatures.**
- **After 3 months of treatment with dupilumab, despite clinical improvement, the blood transcriptome displays residual signs of inflammation, in particular in patients with an eosinophil-high endotype.**

REFERENCES

1. Ewald DA, Malajian D, Krueger JG, Workman CT, Wang T, Tian S, et al. Meta-analysis derived atopic dermatitis (MADAD) transcriptome defines a robust AD signature highlighting the involvement of atherosclerosis and lipid metabolism pathways. BMC Med Genomics 2015;8:1-15.
2. Gittler JK, Shemer A, Suárez-Fariñas M, Fuentes-Duculan J, Gulewicz KJ, Wang CQF, et al. Progressive activation of T_H2/T_H22 cytokines and selective epidermal proteins characterizes acute and chronic atopic dermatitis. J Allergy Clin Immunol 2012;130:1344-54.

3. Tsoi LC, Rodriguez E, Degenhardt F, Baurecht H, Wehkamp U, Volks N, et al. Atopic dermatitis is an IL-13–dominant disease with greater molecular heterogeneity compared to psoriasis. J Invest Dermatol 2019;139:1480-9.
4. Suárez-Fariñas M, Ungar B, Correa Da Rosa J, Ewald DA, Rozenblit M, Gonzalez J, et al. RNA sequencing atopic dermatitis transcriptome profiling provides insights into novel disease mechanisms with potential therapeutic implications. J Allergy Clin Immunol 2015;135:1218-27.
5. Möbus L, Rodriguez E, Harder I, Stölzl D, Boraczynski N, Gerdes S, et al. Atopic dermatitis displays stable and dynamic skin transcriptome signatures. J Allergy Clin Immunol 2021;147:213-23.
6. Sanyal RD, Pavel AB, Glickman J, Chan TC, Zheng X, Zhang N, et al. Atopic dermatitis in African American patients is T_H2/T_H22-skewed with T_H1/T_H17 attenuation. Ann Allergy Asthma Immunol 2019;122:99-110.e6.
7. Esaki H, Brunner PM, Renert-Yuval Y, Czarnowicki T, Huynh T, Tran G, et al. Early-onset pediatric atopic dermatitis is T_H2 but also T_H17 polarized in skin. J Allergy Clin Immunol 2016;138:1639-51.
8. Mack MR, Brestoff JR, Berrien-Elliott MM, Trier AM, Yang TLB, McCullen M, et al. Blood natural killer cell deficiency reveals an immunotherapy strategy for atopic dermatitis. Sci Transl Med 2020;12:eaay1005.
9. Möbus L, Rodriguez E, Harder I, Schwarz A, Wehkamp U, Stölzl D, et al. Elevated NK-cell transcriptional signature and dysbalance of resting and activated NK cells in atopic dermatitis. J Allergy Clin Immunol 2021;147:1959-65.e2.
10. Brunner PM, Suárez-Fariñas M, He H, Malik K, Wen HC, Gonzalez J, et al. The atopic dermatitis blood signature is characterized by increases in inflammatory and cardiovascular risk proteins. Sci Rep 2017;7:1-12.
11. Brunner PM, Silverberg JI, Guttman-Yassky E, Paller AS, Kabashima K, Amagai M, et al. Increasing comorbidities suggest that atopic dermatitis is a systemic disorder. J Invest Dermatol 2017;137:18-25.
12. Hou T, Tsang MSM, Chu IMT, Kan LLY, Hon KL, Leung TF, et al. Skewed inflammation is associated with aberrant interleukin-37 signaling pathway in atopic dermatitis. Allergy Eur J Allergy Clin Immunol 2021;2102-14.
13. Leonard A, Wang J, Yu L, Liu H, Estrada Y, Greenlees L, et al. Atopic dermatitis endotypes based on allergen sensitization, reactivity to *Staphylococcus aureus* antigens, and underlying systemic inflammation. J Allergy Clin Immunol Pract 2020;8:236-47.e3.
14. Huang Y, Chen G, Liu X, Shao Y, Gao P, Xin C, et al. Serum metabolomics study and eicosanoid analysis of childhood atopic dermatitis based on liquid chromatography–mass spectrometry. J Proteome Res 2014;13:5715-23.
15. Brunner PM, Israel A, Leonard A, Pavel AB, Kim HJ, Zhang N, et al. Distinct transcriptomic profiles of early-onset atopic dermatitis in blood and skin of pediatric patients. Ann Allergy Asthma Immunol 2019;122:318-30.e3.
16. Heratizadeh A, Haufe E, Stölzl D, Abraham S, Heinrich L, Kleinheinz A, et al. Baseline characteristics, disease severity and treatment history of patients with atopic dermatitis included in the German AD Registry TREATgermany. J Eur Acad Dermatol Venereol 2020;34:1263-72.
17. Martin M. Cutadapt removes adapter sequences from high-throughput sequencing reads. EMBnet J 2011;17:10; https://doi.org/10.14806/ej.17.1.200.
18. Kim D, Pertea G, Trapnell C, Pimentel H, Kelley R, Salzberg SL. TopHat2: accurate alignment of transcriptomes in the presence of insertions, deletions and gene fusions. Genome Biol 2013;14:R36.
19. Langmead B, Salzberg SL. Fast gapped-read alignment with Bowtie 2. Nat Methods 2012;9:357-9.
20. Li H, Handsaker B, Wysoker A, Fennell T, Ruan J, Homer N, et al. The Sequence Alignment/Map format and SAMtools. Bioinformatics 2009;25:2078-9.
21. Anders S, Pyl PT, Huber W. HTSeq—a Python framework to work with high-throughput sequencing data. Bioinformatics 2015;31:166-9.
22. Frichot E, François O. LEA: an R package for landscape and ecological association studies. Methods Ecol Evol 2015;6:925-9.
23. Zhang Y, Parmigiani G, Johnson WE. ComBat-seq: batch effect adjustment for RNA-Seq count data. NAR Genomics Bioinforma 2020;2:1-10.
24. Leek JT, Johnson WE, Parker HS, Fertig EJ, Jaffe AE, Zhang Y, et al. Sva: surrogate variable analysis. 2021. Available at: https://bioconductor.org/packages/release/bioc/html/sva.html. Accessed February 3, 2022.
25. Lefèvre-Utile A, Saichi M, Oláh P, Delord M, Homey B, Soumelis V, et al. Transcriptome-based identification of novel endotypes in adult atopic dermatitis. Allergy 2021.
26. Kursa MB, Rudnicki WR. Feature selection with the Boruta package. J Stat Softw 2010;36:1-13.
27. Kuhn M. Caret: classification and regression training. 2020. Available at: https://CRAN.R-project.org/package=caret. Accessed February 3, 2022.
28. Love MI, Huber W, Anders S. Moderated estimation of fold change and dispersion for RNA-Seq data with DESeq2. Genome Biol 2014;15:550.
29. Zhu A, Ibrahim JG, Love MI. Heavy-tailed prior distributions for sequence count data: removing the noise and preserving large differences. Bioinformatics 2019;35:2084-92.
30. Yu G, Wang LG, Han Y, He QY. ClusterProfiler: an R package for comparing biological themes among gene clusters. Omi A J Integr Biol 2012;16:284-7.
31. Marwah VS, Kinaret PAS, Serra A, Scala G, Lauerma A, Fortino V, et al. INfORM: Inference of NetwOrk Response Modules. Bioinformatics 2018;34:2136-8.
32. Thul PJ, Akesson L, Wiking M, Mahdessian D, Geladaki A, Ait Blal H, et al. A subcellular map of the human proteome. Science 2017;356:eaal3321.
33. Welte S, Kuttruff S, Waldhauer I, Steinle A. Mutual activation of natural killer cells and monocytes mediated by NKp80-AICL interaction. Nat Immunol 2006;7:1334-42.
34. Bieber T. Atopic dermatitis: an expanding therapeutic pipeline for a complex disease. Nat Rev Drug Discov 2022;21:21-40.
35. Freud AG, Keller KA, Scoville SD, Mundy-Bosse BL, Cheng S, Youssef Y, et al. NKp80 defines a critical step during human natural killer cell development. Cell Rep 2016;16:379-91.
36. Bossel Ben-Moshe N, Hen-Avivi S, Levitin N, Yehezkel D, Oosting M, Joosten LAB, et al. Predicting bacterial infection outcomes using single cell RNA-sequencing analysis of human immune cells. Nat Commun 2019;10:3266.
37. Joehanes R, Johnson AD, Barb JJ, Raghavachari N, Liu P, Woodhouse KA, et al. Gene expression analysis of whole blood, peripheral blood mononuclear cells, and lymphoblastoid cell lines from the Framingham Heart Study. Physiol Genomics 2012;44:59-75.
38. Wong L, Jiang K, Chen Y, Hennon T, Holmes L, Wallace CA, et al. Limits of peripheral blood mononuclear cells for gene expression-based biomarkers in juvenile idiopathic arthritis. Sci Rep 2016;6:29477.
39. He D, Yang CX, Sahin B, Singh A, Shannon CP, Oliveria JP, et al. Whole blood vs PBMC: compartmental differences in gene expression profiling exemplified in asthma. Allergy Asthma Clin Immunol 2019;15:67.